River Water Level and Water Surface Slope Measurement From Spaceborne Radar and LiDAR Altimetry: Evaluation and Implications for Hydrological Studies in the Ganga River

Pankaj R. Dhote, Ankit Agarwal, Gaurish Singhal, Stephane Calmant, Praveen K. Thakur, Hind Oubanas, Adrien Paris, and Raghavendra P. Singh

***Abstract*—Satellite altimetry has revolutionized river monitoring, particularly for hydrologists working on river flow monitoring in sparsely or ungauged areas. Despite this, there is a lack of a comprehensive evaluation of radar and LiDAR altimeters with varying sensor specifications for river water level retrieval, seasonal change characterization, and water surface slope (WSS) using gauged long-term water level and global navigation satellite system data. This study addresses this gap by combined evaluation of radar (ENVISAT to Sentinel-3) and LiDAR (ICESat-1, ICESat-2) altimeters along the Ganga River, from Prayagraj to Varanasi. We found that all the radar altimetry missions showed better accuracy for water level retrievals ($R^2 >= 0.8$; RMSE 0.11 to 1.16 m) and water level change quantification (RMSE 0.59 m). However, Sentinel-3 with synthetic aperture radar (SAR) acquisition mode outperformed (RMSE 0.11 to 0.14 m) all the radar missions having low resolution mode. Despite LiDAR missions' high vertical accuracy, they show relatively lower accuracy in water level time series generation due to nonrepeating characteristics. In contrary, ICESat-2 demonstrates potential in capturing spatial and seasonal variability of WSS, enhancing the accuracy of surface water and ocean topography (SWOT) discharge products when combined with SWOT River database. This study provides a comprehensive baseline for end-users interested in utilizing radar and LiDAR missions for various hydrological applications, including river discharge estimation. Moreover, the studied river reach shares the SWOT calibration orbit, allowing the utilization of generated satellite and in-situ databases for the effective evaluation of SWOT measurements.**

***Index Terms*—Ganga river, ICESat-2, LiDAR altimetry, radar altimetry, remote sensing, surface water and ocean topography (SWOT) mission.**

Manuscript received 27 December 2023; revised 11 February 2024; accepted 3 March 2024. Date of publication 20 March 2024; date of current version 12 April 2024. This work was supported in part by the Indian Space Research Organization Project under Grant TDP2023-2026, in part by the Indian Institute of Technology, Roorkee under Grant HYDRO-Flood, and in part by the Helmholtz Centre for Geosciences GFZ Potsdam section 4.4 for the Article Processing Charges. *(Corresponding authors: Pankaj R. Dhote; Ankit Agarwal.)*

Pankaj R. Dhote is with the Department of Hydrology, Indian Institute of Technology, Roorkee 247667, India, also with the Water Resources Department, Indian Institute of Remote Sensing, ISRO, Dehradun 248001, India, and also with the G-EAU, Univ Montpellier, AgroParisTech, BRGM, CIRAD, IRD, INRAE, Institut Agro, 34196 Montpellier, France (e-mail: pankaj_d@hy.iitr.ac.in).

Ankit Agarwal is with the Department of Hydrology, Indian Institute of Technology, Roorkee 247667, India, and also with the GFZ German Research Centre for Geosciences, Helmholtz Centre, Potsdam, Germany (e-mail: ankit.agarwal@hy.iitr.ac.in).

Gaurish Singhal, Praveen K. Thakur, and Raghavendra P. Singh are with the Water Resources Department, Indian Institute of Remote Sensing, ISRO, Dehradun 248001, India (e-mail: gaurishsinghal@gmail.com; praveen@iirs.gov.in; rpsingh@iirs.gov.in).

Stephane Calmant is with the LEGOS, Université de Toulouse, CNRS-IRD-UPS-CNES, 31400 Toulouse, France (e-mail: stephane.calmant@ird.fr).

Hind Oubanas is with the G-EAU, Univ Montpellier, AgroParisTech, BRGM, CIRAD, IRD, INRAE, Institut Agro, 34196 Montpellier, France (e-mail: hind.oubanas@inrae.fr).

Adrien Paris is with the Hydro-Matters, 31460 Le Faget, France (e-mail: adrien.paris@hydro-matters.fr).

This article has supplementary downloadable material available at https://doi.org/10.1109/JSTARS.2024.3379874, provided by the authors.

Digital Object Identifier 10.1109/JSTARS.2024.3379874

I. Introduction

MONITORING of inland water is essential in evaluating various components of hydrological cycle, environmental and atmospheric processes of the earth system. The understanding of hydrological processes and management of water resources, as well as ecosystem balance, heavily relies on monitoring water level variations [1]. Traditionally, water level has been monitored using in situ gauging stations, but the existing deployed networking of spatially distributed stations is limited on a global scale due to cost, accessibility, and economical/political issues [2], [3], [4]. In addition, the availability of global in situ stations has been decreasing in the past decades [5], [6]. Therefore, there is an uprising trend in the use of satellite observations for globally monitoring of water levels. Over the past 25 years, satellite radar altimetry has emerged as a valuable alternative for obtaining water surface elevation (WSE) observations [7]. These observations are obtained at virtual stations (VSs), which are formed at the locations where satellite tracks cross a river. Moreover, the recently launched (December 15, 2022) surface water and ocean topography (SWOT) mission promises to give measurements of water surface elevation, river width and slope globally [8].

Satellite altimetry has proven to be highly effective for global-scale monitoring of inland water bodies. Two types of satellite altimeters are available: radar and laser altimeters. Significant advancements have been made in the specifications of radar altimeter sensors in last two decades [7]. The use of Ka-band, rather than Ku-band, in the Saral/AltiKa mission in 2013 resulted in higher bandwidth and a smaller footprint [9]. Synthetic

aperture mode (SAR) has been implemented in recent missions such as Sentinel 3, Cryosat 2, and Sentinel 6, allowing for small footprint sampling in the along-track direction. To improve data quality and increase observation rates, various retracking algorithms have been developed using high-rate altimetry data [10], [11], [12]. To improve spatial and temporal resolution, attempts have been made to generate combined water level time series from multimission data operating at the same or different orbits (Topex-Poseidon, Jason1/2/310 days; Saral/AltiKa 35 days; Sentinel-327 days) [13], [14], [15]. The generated altimetry-based water level time-series have been used to estimate river discharge and to calibrate hydrological–hydrodynamic models [16], [17], [18], [19], [20], [21]. Several studies have demonstrated the usefulness of satellite altimetry in constructing river water level time series for large river basins such as the Amazon, Ganga, and Brahmaputra [22], [23], [24]. While there have been efforts to use multimission altimetry data to study lake and wasteland dynamics, there has been relatively limited research to assess seasonal changes in river water levels [25], [26], [27], [28]. As a result, it is crucial to focus on accurately capturing river water level variations in both time and space using satellite altimetry data.

Radar altimetry provides elevation measurements of the earth's surface only in the nadir direction, resulting in limited coverage of the earth's surface. To increase the number of water bodies where water level can be retrieved, LiDAR missions have been used as they have a small footprint (approximately 70 m for Ice, Cloud, and Land Elevation Satellite-ICESat and 17 m for ICESat-2) and a long-periodic orbit that allows for observation of a larger part of the earth's surface at the relatively low temporal resolution [29], [30], [31]. The Geoscience Laser Altimeter System (GLAS), the first spaceborne LiDAR altimeter, was launched by NASA in January 2003 onboard the ICESat mission and the advanced topographic laser altimeter system (ATLAS) was launched on the follow-up ICESat-2 mission by NASA in 2018 [32], [33]. Although primarily designed for glacier, sea-ice, and vegetation structure observation, these altimeters have demonstrated potential in inland water level observation [31], [34], [35]. The LiDAR altimeters have coarse temporal resolution (91 days) and do not produce repeat measurements at the same location, making it difficult to capture high water level fluctuations in rivers. Consequently, application of LiDAR data is more common in lakes monitoring compared to river water levels. In addition, ICESat-2 has been exploited to estimate water surface slope (WSS) [36]; which is essential parameter for river discharge estimation. The SWOT a priori river database (SWORD) archives WSS as river reach attribute which is important for SWOT products generation [37]. This further emphasizes the need to evaluate the performance of ICESat-2 data for WSS estimation using in situ measurements.

Diverse techniques for data collection and processing can introduce varying degrees of error into elevation results obtained through altimetry. As a result, validating against gauge data becomes essential to ensure the reliability of extracted water levels. Multiple investigations have been conducted to assess the precision of radar altimeters over inland water bodies across different global regions. For instance, Envisat altimetry data showed root-mean-square error (RMSE) values spanning between 0.32 and 0.72 m, 0.46 and 0.99 m, and 0.5 and 1.6 m when compared against in situ measurements at distinct virtual stations in the Zambezi, Brahmaputra, and Garonne river basins, respectively [20], [38], [39]. A study by Schneider et al. [40] exploited CryoSat-2 data along the Po River, resulting in an average RMSE of 0.38 m. The findings were also leveraged to calibrate the channel roughness coefficient in a hydrodynamic model. Kittel et al. [41] evaluated the suitability of Sentinel-3A/3B for monitoring river water levels in the Zambezi river basin, revealing RMSE deviations ranging from 2.9 to 31.3 cm across six virtual stations. Furthermore, Chen et al. [42] combined water level measurements derived from Sentinel-3A data using five different retracking algorithms against in situ measurements. The study found median RMSE values spanning from 0.46 to 0.82 m at virtual stations.

The evaluation of LiDAR altimeter performance for rivers encounters limitations due to the distinctive nature of nonrepeated track measurements and coarse temporal resolution, differing from conventional fixed gauging systems employed for river monitoring. Consequently, several investigations have focused on assessing the efficacy of LiDAR altimeters concerning lakes and reservoirs [25], [28]. The study by Jarihani et al. [16] over Australia's Lake Argyle revealed that ICESat showed better performance compared to Jason-2. Frappart et al. [34] conducted an assessment of ICESat-2's capabilities across ten Swiss lakes and discovered its remarkable accuracy (RMSE $<$ 0.6 m) in relation to gauge data. Within the context of the Mississippi River, an extensive network of in situ measurements facilitated the evaluation of ICESat, ICESat-2, and GEDI data [28]. The study disclosed that ICESat-2 (RMSE 0.12 m) provided more dependable water level information compared to ICESat (RMSE 0.25 m) and GEDI (RMSE 0.4 m). While evaluating the ICESat-2 over Ohio River, it is observed that that ICESat-2 can resolve and measure rivers as narrow as 6 m. RMSE of retrieved river levels ranges between 0.19 and 0.25 m for rivers narrower than 50 m, and from 0.08 to 0.15 m for those wider than 50 m, with averages of 0.24 and 0.12 m, respectively [43].

Past research has assessed the effectiveness of altimetry missions at diverse virtual stations. However, there remains a limited comprehension regarding the performance of both radar and LiDAR altimeters within the same river stretch, utilizing measurements from gauges and global navigation satellite system (GNSS) observations. The novelty of the present work lies in approaches that evaluate radar and LiDAR altimeters comprehensively, while encompassing several key considerations, which are as follows:

1) acquisition mode and frequency;
2) potential of radar altimeters in discerning seasonal water level fluctuations;
3) potential of LiDAR altimeter (ICESat-2) for WSS estimation.

This study integrates water level measurements from eight spaceborne satellites—six equipped with radar altimeters and two with LiDAR altimeters—launched after 2000. The main objectives of this study are as follows:

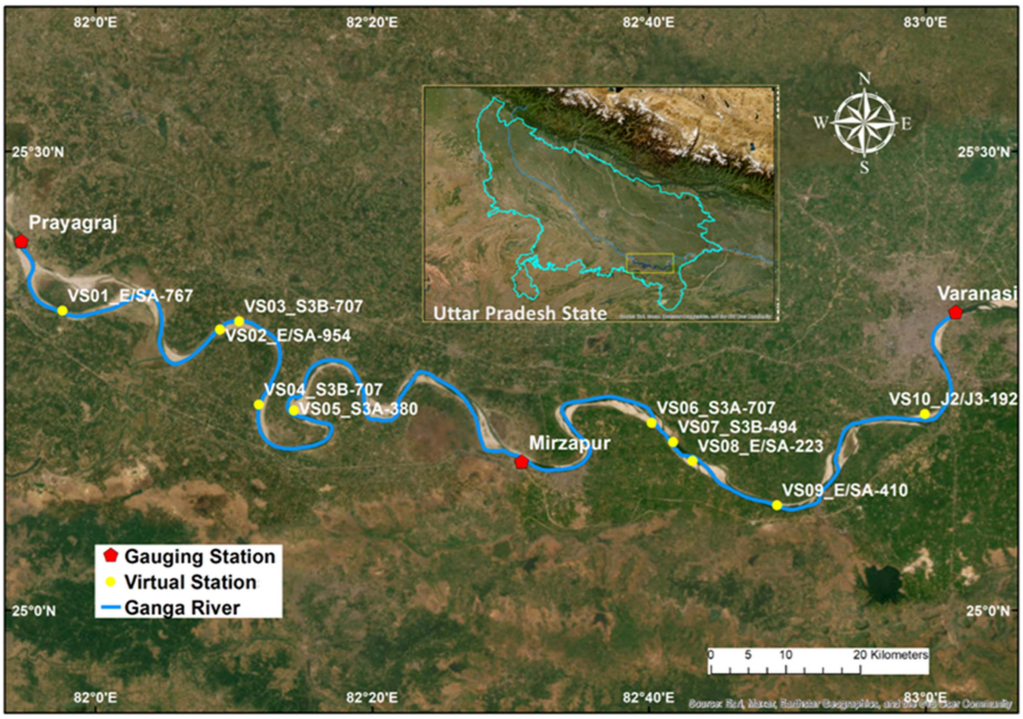

Fig. 1. Ganga River stretch (Prayagraj to Varanasi) considered in the study along with locations of gauging stations and identified virtual stations (VSs) from multimission radar altimetry data (background image credits: Esri, DigitalGlobe, GeoEye, earthstar geographics, CNES/Airbus DS, USDA, USGS, AEX, getmapping, aerogrid, IGN, IGP, swiss topo, and the GIS user community). White color label corresponding to each virtual station represents station number and data type [Envisat (E), Jason 2 (J2), Jason 3(J3), SARAL/AltiKa (SA), Sentinel 3A (S3A), and Sentinel 3B (S3B)].

1) conducting a performance assessment of radar altimeters (from ENVISAT to Sentinel-3) and LiDAR altimeters (ICESat, ICESat-2) for generating water level time-series;
2) examining radar altimetry data to characterize seasonal changes in water levels;
3) appraising ICESat-2 data's suitability for estimating WSS and conducting a comparative analysis with WSS derived from SWORD.

II. Study Area and Data

A. Study Area

The research focus of this study is the ∼210 km segment of the Ganga River that spans from Prayagraj to Varanasi in Uttar Pradesh, India, as shown in Fig. 1. The Ganga River is a vital source of surface water and groundwater for 11 states in India, including Uttar Pradesh. It is the largest basin in India, covering 861 452 sq. km, and originates from the North West Himalayas in Uttarakhand State, flowing approximately 2525 km until Farakka station. The river is used for various purposes, such as drinking, hydropower generation, irrigation, and industrial activities [44]. The selected segment of the river is also part of the national waterway NW-1 (Prayagraj to Haldia), which requires a minimum amount of draft to facilitate the movement of traffic. The study area has a main channel width ranging from ∼200 to ∼1000 m, and the lateral floodplain extends up to ∼7.5 km. The locations of the gauging stations and VSs considered in this study are depicted in Fig. 1. The Ganga River presents an ideal test site to assess the performance of altimetry products, given the importance of the river as it provides water to one-third population of India [45], its religious significance, and the frequent flooding experienced by villages and towns located on both banks of the river.

B. Data

1) Radar Altimetry Data: Table I presents an overview of various radar altimetry missions, namely Envisat, SARAL/AltiKa, Jason-2, Jason-3, Sentinel-3A, and Sentinel-3B, which are considered in the present work. The source of data is Hydroweb and Center for Topographic Studies of the Ocean and Hydrosphere [46]. These missions have different sensor characteristics resulting in differences in the spatial–temporal resolution and accuracy. Specifically, Envisat, SARAL/AltiKa, Jason-2, and Jason-3 operate in low resolution mode (LRM), while Sentinel-3A and Sentinel-3B use synthetic aperture radar (SAR) mode. In addition, Envisat, Jason-2, Jason-3, Sentinel-3A, and Sentinel-3B operate at Ku-band frequency, while SARAL/AltiKa operates at Ka-band frequency. In terms of temporal resolution, the majority of the missions considered in this study have a low temporal resolution. The Envisat and SARAL/AltiKa have a revisit time of 35 days, while Sentinel-3A and Sentinel-3B have a revisit time of 27 days. In contrast, Jason-2 and Jason-3 provide water surface elevation measurements every ten days.

With regards to orbit configurations, Envisat, which was active from May 2002 to October 2010, and SARAL/AltiKa, which was active from March 2013 to July 2016, succeeded the ERS-2

TABLE I
SENSOR SPECIFICATIONS AND ALTIMETRY TIME-SERIES CONSIDERED IN THE STUDY

Mission	Temporal Resolution (day)	Height (km)	Inclination (degrees)	Observation Period	Source
Radar Altimetry					
ENVISAT	35	800	98.5	2002–2010	Hydroweb /CTOH
Jason 2	9.91	1336	66	2008–2015	Hydroweb /CTOH
Jason 3	10	1336	66	2016–2019	Hydroweb /CTOH
SARAL/AltiKa	35	800	98.5	2013–2016	Hydroweb /CTOH
Sentinel 3A	27	814.5	95.65	2016–2019	Hydroweb /CTOH
Sentinel 3B	27	814.5	95.65	2018–2019	Hydroweb /CTOH
Lidar Altimetry					
ICESat	91	600	94	2003–2009	NSIDC
ICESat-2	91	496	92	2018–2022	NSIDC

mission (active from April 1995 to September 2007) and used the same orbit configuration with an intertrack distance of 80 km at the equator. Jason-2, launched in June 2008, and its successor Jason-3, launched in 2016, were placed in the same orbit with an intertrack distance of approximately 315 km at the equator. Currently active, the Sentinel-3 mission provides SAR altimetry data with a revisit time of 27 days. The two Sentinel-3 satellites have orbits that are almost identical to those of Envisat and SARAL/AltiKa, with a ground-track separation of 104 km at the equator.

The data from Envisat and SARAL/AltiKa are processed using the ICE-1 retracker, while Jason-2 and Jason-3 are processed using the ICE retracker [47], [48], [49]. The OCOG retracker, a derivative of ICE-1, is used to process data from Sentinel-3A and Sentinel-3B, which is suitable for inland applications. The retrieved water levels from all the missions corresponds to high-rate altimetry datasets with a standard rate of 20 Hz, which leads to a distance of 294 m along the track between successive measurements. However, the Saral/AltiKa dataset has a higher sampling rate of 40 Hz, resulting in a smaller spatial spacing of 173 m along the track.

2) LiDAR Altimetry Data: In this study, we used LiDAR altimeter data from two satellites, i.e., ICESat and ICESat-2 (see Table I). The geoscience laser altimeter system (GLAS) onboard the ICESat is the first spaceborne laser altimeter, operating at green (532 nm) and near-infrared (1064 nm) wavelengths and emitting laser pulses data at 40 Hz (40 points per sec). The mission was launched by NASA in January 2003 [32], [50] and stopped collecting data in the year 2009. The near-infrared channel was used for surface altimetry (i.e., elevation measurement in land, ice sheet, sea ice, and ocean), while green channel was used for vertical distribution of aerosols and clouds [51]. GLAS had a footprint of 70 m diameter with along track spacing of 172 m. Various datasets have been produced from GLAS, covering all campaigns, for scientific community. In this study, we used GLA14 (GLAS/ICESat L2 Global Land Surface Altimetry Data, Version 34) product. The data were downloaded from National Snow and Ice Data Center (NSIDC) for a period from February 2003 to October 2009.

In continuation with ICESat, NASA launched the ICESat-2 mission in September 2018 which is currently still active. ICESat-2 carries ATLAS, operating at green wavelength (532 nm) and emits pulses at 10 kHz which corresponds to 250 times of the ICESat mission leading to improved along track sampling at the interval of 0.7 m [52]. In contradiction to full waveform system, ATLAS uses photon detectors to determine the range of the target features on earth surface. The diffractive optical element used in the system splits outgoing single laser beam into three pairs of beams (90 m distance within the pairs) spaced approximately 3.3 km apart, each consisting of one high-energy beam and one low energy beam [33]. Finally, each beam (out of six beams) can be identified by its orientation (left-L; right-R) and laser spot number (1 to 3; e.g., GT1L/GT1R, GT2L/GT2R, and GT3L/GT3R). This multibeam configuration enables targeting surfaces with wider range of reflectivity and estimate local terrain slope. The ICESat-2 laser has footprint diameter of 17 m generating an overlap in footprints. ICESat-2 mission has developed various geophysical products such as land ice (ATL06), sea ice (ATL07), land/vegetation (ATL08), atmosphere (ATL09), oceans (ATL12), and inland water (ATL03/ATL13). In this work, ATL13 products from October 2018 to July 2022 was used by downloading data from NSIDC.

3) Field Campaign and In Situ Data: We conducted a field survey to collect continuous river water surface elevation

Fig. 2. Field survey conducted in Ganga river. (a) River water surface elevation measurement using GNSS carpet. (b) GCPs collection at river gauging sites. (c) and (d) field preparation.

data from Prayagraj to Varanasi using GNSS Carpet (Trimble NetR9). Two field campaigns were conducted during monsoon (October 2–5, 2022) and nonmonsoon (April 23–26, 2023) seasons to account for seasonal variability of WSS (see Fig. 2). The GNSS carpet was tied behind the motorized boat separated by a distance of 10–15 ft to avoid disturbances imposed by the boat. Furthermore, we collected GCPs using other GNSS system (Leica GS10) at gauging sites for estimation of datum correction required to convert observed in situ water levels from mean sea level of India datum to EGM 2008 datum.

Water level records from in situ gauge stations (Prayagraj and Varanasi) at daily time-step over Ganga River were made available by the Central Water Commission (CWC), India (see Fig. 1 for their location) for the period January 2000 to May 2019.

III. Methodology

A. Water Level Time-Series Generation Using Multimission Altimetry Data

1) Radar Altimetry Data Processing: We followed two step procedure to generate water level time-series from the radar altimetry data. First, we downloaded data from the Hydroweb platform[1] [53]. In the second step, raw data were downloaded from CTOH after filling the request form to overcome the data gaps observed in Hydroweb data [46]. These downloaded data were processed using open-source python-based altimetry time series software (AlTiS). The software is developed by CTOH, which is a French observation service working for altimetry studies. The graphical user interface of AlTiS facilitates to process all the radar altimetry data used in the study, i.e., Envisat, SARAL/AltiKa, Jason-2, Jason-3, Sentinel-3A, and Sentinel-3B. Water level time-series were generated by creating polygons for each virtual station so that the corresponding footprints within the river channel can be fetched. Outlier points that are not following the trend were removed via iterative process by computing median absolute deviation and standard deviation. The multitemporal data of respective mission were processed individually. All the retrieved water levels from multisatellites were referenced to EGM 2008 datum.

2) LiDAR Altimetry Data Processing: The water levels from Prayagraj to Varanasi using LiDAR altimeters (ICESat and

[1][Online]. Available: https://hydroweb.theia-land.fr/

ICESat-2) are provided by NSIDC by incorporating atmospheric and geophysical corrections. The OpenAltimetry website[2] [54], NASA funded project of Scripps Institution of Oceanography, San Diego Supercomputer Center, NSIDC, and UNAVCO facilitate visualization of the laser altimetry data track-wise and can be used to export the data in CSV. Each track from GLA14 product of ICESat and ATL13 of ICESat-2 composed of photon data with precise latitude, longitude, and elevation arranged in along-track direction. We used the fly option to visualize the elevation profile of each track within the selected boundary box, which helped to exclude outliers and export reliable data. Later, exported data were averaged to generate water level, which further involved the detection and removal of outliers based on standard deviation of single measurement. OpenAltimetry provides ICESat/GLS14 data with reference to WGS 84 ellipsoid vertical datum. We converted the retrieved water heights to EGM 2008 by applying geoidal correction using UNAVCO geoidal calculator.[3] No geoidal correction was applied to ATL13, as it is already available with EGM 2008 datum.

B. Evaluation and Analysis of Altimetry-Derived Water Levels and Water Surface Slope (WSS)

As the virtual stations do not correspond to the exact location of gauging stations (see Fig. 1), the direct evaluation is difficult especially in basins where the density of gauging network is very poor. To tackle this problem, first we applied datum correction to in situ water levels using GCPs to convert them from local mean sea level to common EGM 2008 datum. Second, we used linearly interpolated in situ water surface height at virtual stations using upstream and downstream gauging stations [19], [55], [56]. The method looks reliable considering the relatively flat terrain and no hydraulic structures within the selected reach. Finally, the interpolated river water levels were used to validate the radar altimetry derived measurements. However, it is more complicated when it comes to LiDAR altimeters due to not repeat-measurements along the track. In this case, we had to shift the water surface heights on the location of respective tracks before performing evaluation at virtual stations. We used statistical indicators such RMSE, Nash–Sutcliffe efficiency (NSE), and coefficient of determination (R^2) for performance evaluation analysis. These indicators were selected considering their utilization and reliability in similar previous works [19], [25], [28]. Furthermore, we examined the potential of radar altimetry-derived water level time-series for seasonal water level changes analysis using in-situ data.

To assess the performance of ICESat-2 WSS from Prayagraj to Varanasi, we used observations from gauging stations and GNSS data and compared with SWORD database. First, we assessed the GNNS-based WSS spatial variations at virtual stations during monsoon and nonmonsoon season. Second, we estimated the WSS using ICESat-2 data pairs during dates that are relatively close (within 4–5 days), ensuring that the satellite overpasses the desired stretch, albeit near the ends of the stretch. This approach allows for obtaining an overall WSS for the entire stretch. Finally, comparative assessment was also carried out corresponding to SWORD river reaches.

[2][Online]. Available: https://openaltimetry.org/

[3][Online]. Available: https://www.unavco.org/software/geodetic-utilities/geoid-height-calculator/geoid-height-calculator.html

IV. Results

A. Accuracy of Radar and LiDAR Altimetry Data Over Ganga River

Table II presents a comprehensive summary of the accuracy metric when comparing radar altimetry and in situ water level time-series at ten virtual stations. Among these stations, five have common observations with two separate satellite altimetry missions. The table reports the number of observations (n) that constitutes each time series, R^2, mean difference (MD or bias), RMSE, and NSE. Altimetry products are listed in a chronological order as per the assigned virtual station number as given in Fig. 1. In the case of VSs observed from multiple sensors (e.g., VS1, VS2), the performance evaluation has been performed for each time series and combined virtual station.

In Table II, all altimetry series demonstrate notably elevated R^2 values, consistently exceeding 0.8 across various historical to recent missions. The RMSE at ten virtual stations ranged from 0.11 to 1.16 m. The NSE values exhibit positivity at every virtual station, consistently surpassing 0.64. Remarkably, despite having the fewest observations, the S3B mission surpasses all other missions in terms of performance, yielding the lowest RMSE values at VS3, VS4, and VS7—measuring 0.14, 0.11, and 0.12 m, respectively. Adjustments for bias (altimetry—in situ) were implemented at each station, spanning from 0.09 to 1.55 m. Across the observation span, the E and SA series closely mirror the performance exhibited by S3A and S3B, except for SA at VS2, which resulted in an RMSE of 1.16 m. Furthermore, the J2 and J3 series at virtual station 10 displayed relatively higher RMSE values of 1.11 and 0.98 m, respectively, despite having a greater number of observations. In a broader context, the performance indices exhibit a consistent pattern from Prayagraj to Varanasi along the Ganga River. This homogeneity underscores the robustness of the altimetry data's precision and reliability across this geographical span.

Table III provides a concise summary of the accuracy metrics derived from ICESat and ICESat-2 data analyses conducted over the Ganga River. For LiDAR altimetry-based water level time-series, nine virtual stations were identified for ICESat (see Fig. 3). However, for ICESat-2, the evaluation was performed at a river scale due to the limited sample size and absence of repetition. The ICESat observations were consistent with the in situ data with $R^2 >= 0.6$ at three stations only out of nine. The average RMSE was found to be 0.82 m having range from 0.58 to 1.07 m. Conversely, at the river scale, ICESat-2 measurements yielded an RMSE of 0.64 m. The NSE for ICESat measurements varied between –1.31 and 0.77, with NSE values exceeding or equal to 0.5 recorded at two stations exclusively. In contrast, ICESat-2 measurements exhibited an NSE of 0.97 at the river scale. Overall, ICESat-2 measurements marked a better accuracy over ICESat within limited data availability.

TABLE II
ACCURACY METRICS OF MULTIMISSION RADAR ALTIMETRY DATA AT TEN VIRTUAL STATIONS

Virtual Station	Distance (km)	*N*	R^2	RMSE	NSE	Bias Correction (m)
VS1 E/SA	11.14	109	0.97	0.41	0.96	0.9
VS1 E-767	11.14	77	0.98	0.34	0.97	0.9
VS1 SA-767	11.14	32	0.97	0.56	0.95	0.9
VS2 E/SA	39.50	69	0.92	0.88	0.88	0.18
VS2 E-954	39.50	53	0.93	0.78	0.89	0.18
VS2 SA-954	39.50	16	0.89	1.16	0.84	0.18
VS3 S3B-707	42.22	7	0.82	0.14	0.65	1
VS4 S3B-707	55.83	7	0.89	0.11	0.78	0.38
VS5 S3A-380	75.08	41	0.96	0.65	0.91	0.09
VS6 S3A-707	150.76	43	0.96	0.52	0.95	0.83
VS7 S3B-494	154.07	7	0.92	0.12	0.72	0.53
VS8 E/SA	157.69	108	0.93	0.62	0.92	1.55
VS8 E-223	157.69	76	0.95	0.59	0.92	1.55
VS8 SA-223	157.69	32	0.98	0.68	0.91	1.55
VS9 E/SA	169.52	77	0.95	0.59	0.77	1.03
VS9 E-410	169.52	46	0.97	0.52	0.64	1.03
VS9 SA-410	169.52	31	0.96	0.68	0.8	1.03
VS10 J2/J3	194.66	358	0.9	1.08	0.79	0.61
VS10 J2-192	194.66	248	0.88	1.11	0.77	0.61
VS10 J3-192	194.66	110	0.94	0.98	0.82	0.61

TABLE III
ACCURACY METRICS OF LiDAR ALTIMETERS

Virtual Station	Distance (km)	*N*	R^2	RMSE	NSE	Bias Correction (m)
ICESat						
VS1_ICE-79	13.396	5	0.179	0.69	−1.31	–
VS2_ICE-213	34.480	14	0.751	0.63	0.36	−2.076
VS3_ICE-176	65.056	11	0.655	0.75	0.46	–
VS4_ICE-176	72.514	11	0.566	1.02	0.50	–
VS5_ICE-176	77.327	9	0.469	0.91	0.14	–
VS6_ICE-42	94.576	5	0.830	1.07	0.77	–
VS7_ICE-1195	136.931	1	–	–	–	–
VS8_ICE-332	170.043	13	0.331	0.873	0.24	–
VS9_ICE-295	201.866	13	0.581	0.580	0.229	0.73
ICESat-2	–	**19**	**0.97**	**0.64**	**0.97**	–

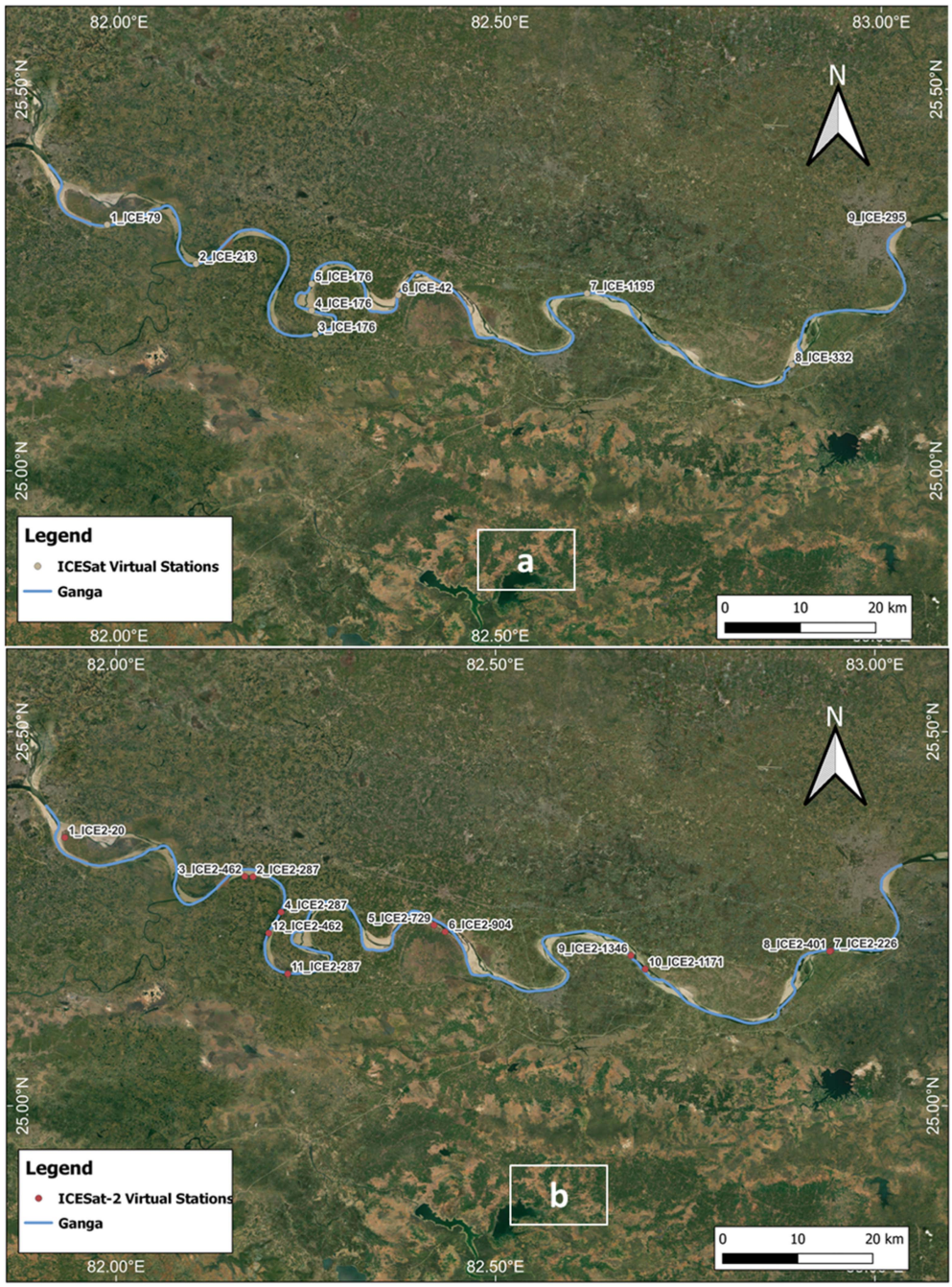

Fig. 3. Identified ICESat (a) and ICESat-2 (b) virtual stations along Ganga river from Prayagraj to Varanasi. ICESat-2 stations do not follow spatially sequential names, as these are defined based on timescale.

B. Water Level Change Analysis Using Radar Altimetry Data

In this section, we assess the potential of radar altimetry-derived water level time-series for analyzing seasonal fluctuations in water levels at individual virtual stations. Table IV provides an overview of the change in average water levels between the premonsoon (March–June) and monsoon (July–October) periods at each station using both altimetry observations and in situ measurements. The investigation reveals that regardless of the station's location and the observed time frequency, the variation in water levels spans from 4.01 to 5.25 m for altimetry data and 4.02 to 4.34 m for in situ data. The RMSE associated with changes in water levels was determined to be 0.59 m. Minimal disparity is observed between the altimetry-derived (4.61 m) and in situ-based (4.13 m) average alterations in water levels between the premonsoon and monsoon seasons. The statistical assessment underscores the close correspondence between these two approaches, affirming capability of radar altimetry in capturing seasonal water level dynamics.

C. Accuracy of Estimated Water Surface Slope

The WSS holds a pivotal role in hydraulic analyses of river systems. Traditionally, gauges have been used to determine WSS

TABLE IV
SEASONAL WATER LEVEL FLUCTUATIONS OBSERVED USING ALTIMETRY AND IN-SITU DATA

		Altimetry			In-Situ		
Virtual Station	**Time Period**	**Avg. Pre-Monsoon WL (m)**	**Avg. Monsoon WL (m)**	**Change in WL (m)**	**Avg. Pre-Monsoon WL (m)**	**Avg. Monsoon WL (m)**	**Change in WL (m)**
VS1 E/SA-767	2002–2016	71.67	76.03	4.36	70.91	75.02	4.11
VS2 E/SA-954	2002–2016	68.71	73.2	4.49	69.23	73.34	4.11
VS3 S3B-707	2018–2022	68.5	73.28	4.78	69	73.01	4.02
VS4 S3B-707	2018–2022	68.39	73.01	4.62	68.19	72.21	4.02
VS5 S3A-380	2016–2022	67.2	71.84	4.64	66.88	71.22	4.34
VS6 S3A-707	2016–2022	63.59	68.11	4.52	62.41	66.75	4.34
VS7 S3B-494	2018–2022	63.46	68.54	5.08	62.39	66.4	4.02
VS8 E/SA-223	2002–2016	63.71	67.72	4.01	62.25	66.36	4.1
VS9 E/SA-410	2002–2016	62.45	66.79	4.34	61.55	65.66	4.11
VS10 J2/J3-192	2008–2022	60.35	65.6	5.25	60.06	64.25	4.19

for river reaches. Conversely, satellite observations, harnessing digital elevation models (DEMs), have been employed as an alternative to estimate WSS over extensive stretches of rivers. However, the WSS derived from DEMs represents the specific day of observation and limiting its application for assessment of seasonal variability [57]. With the emergence of satellite altimetry, small-scale slopes have gained significance due to their usefulness in adjusting altimetry-based water surface elevation readings from one station to another, thus enhancing the density of the water surface elevation time series [13], [58]. ICESat-2, equipped with a unique configuration of six beams and a small footprint of 17 m, has proven effective in determining the instantaneous WSS for approximately a 6 km stretch lying between the beams [36]. We used the following three steps approach to assess the performance of WSS using ICESat-2 along Ganga River.

1) WSS Using GNSS at Virtual Stations: The WSE measurements, gathered during field campaigns conducted in April 2023 (nonmonsoon) and October 2022 (monsoon), is used to calculate the WSS. These slopes were determined by calculating the difference in elevation between the starting point of the river stretch (CWC Gauge at Prayagraj) and the positions of virtual stations (Microwave + LiDAR) as indicated in Supplement Tables A, B, and C. Through these two campaigns, we obtained WSS values for both the monsoon and nonmonsoon seasons, revealing variations in WSS attributed to seasonal changes. This process facilitated an assessment of spatial and seasonal fluctuations in WSS. Overall, we noticed that the WSS during the nonmonsoon season tended to be higher compared to the monsoon season at various virtual stations.

By considering the final virtual station of the radar and LiDAR stations, we estimated the average WSS for the entire stretch to be 6.03 cm/km for the monsoon season and 6.17 cm/km for the nonmonsoon season. A comparison between WSS values derived through GNSS and the long-term seasonal slope calculated from in situ gauge data is presented in Table V. This comparison clearly illustrates a disparity between the two approaches. This difference can be attributed to the fact that GNSS readings pertain to the specific survey day, while the WSS derived from in situ gauges represents long-term averages from daily observations.

2) WSS Using ICESat-2 Data on River Scale: The WSS was determined for the whole stretch using the date pair technique as mentioned in Section III-B. The specific locations and particulars of these date pairs are illustrated in Table VI and Fig. 4. A total of 16 pairs were identified, encompassing data from the years 2019 to 2022. In these cases, strong beams were employed to extract elevation information. The ATL03 geolocated photon data were superimposed onto the map displaying the average water extent of the river. By aligning the river reach's centerline with the overlaid photon data along the track, elevation values were extracted. The calculation of WSS was performed by dividing the difference in elevation by the distance corresponding to the changing pairwise point data over time (refer to Table VI). This methodology provided us with seasonal slopes for both the monsoon and nonmonsoon seasons.

TABLE V
COMPARISON OF GNSS-BASED WSS AT VIRTUAL STATIONS AND IN SITU DATA

GNSS WSS at virtual stations	Monsoon slope (cm/km)	Nonmonsoon slope (cm/km)
Radar Altimeters	5.9	6.13
ICESat	6.07	6.07
ICESat-2	6.13	6.31
Average of GNSS-based WSS	**6.03**	**6.17**
Long-term in-Situ WSS	**5.32**	**5.75**
Mean absolute error (GNSS-based average – in-situ)	**0.71**	**0.42**

TABLE VI
SLOPE DETERMINED USING ICESAT-2 PHOTON DATA

air	Date	Latitude	Longitude	Difference: Elevation (m)	Difference: Distance (km)	Slopes (cm/km)	Season
1	October 11, 2021	25.26909	82.30142	5.49	105.54	5.2	Monsoon
1	October 7, 2021	25.221	83.02156	0	0	0	Monsoon
2	January 17, 2022	25.20785	82.93679	8.05	138.73	5.8	Nonmonsoon
2	January 21, 2022	25.31633	82.16991	0	0	0	Nonmonsoon
3	July 6, 2022	25.11319	82.85461	6.32	130.80	4.83	Monsoon
3	July 10, 2022	25.28406	82.12253	0	0	0	Monsoon
4	April 22, 2022	25.17645	82.23634	7.01	120.64	5.81	Nonmonsoon
4	April 18, 2022	25.20997	82.96946	0	0	0	Nonmonsoon
5	March 26, 2019	25.19954	82.67887	9.09	142.91	6.36	Nonmonsoon
5	March 30, 2019	25.38719	81.91788	0	0	0	Nonmonsoon
6	October 15, 2019	25.3475	82.05029	6.59	159.35	4.14	Monsoon
6	October 11, 2019	25.20766	82.94213	0	0	0	Monsoon
7	November 9, 2019	25.31879	83.02672	6.87	112.29	6.12	Nonmonsoon
7	November 13, 2019	25.2307	82.32289	0	0	0	Nonmonsoon
8	January 14, 2020	25.31429	82.18514	7.83	141.15	5.55	Nonmonsoon
8	January 10, 2020	25.20914	82.97516	0	0	0	Nonmonsoon
9	April 10, 2020	25.11637	82.85429	6.59	130.88	5.04	Nonmonsoon
9	April 14, 2020	25.28409	82.12232	0	0	0	Nonmonsoon
10	July 21, 2020	25.20835	82.93636	7.58	135.28	5.60	Monsoon
10	July 25, 2020	25.30724	82.20084	0	0	0	Monsoon
11	September 21, 2020	25.20231	82.67632	8.36	142.77	5.86	Monsoon
11	September 25, 2020	25.3884	81.9186	0	0	0	Monsoon
12	October 20, 2020	25.20964	82.9687	7.38	138.66	5.32	Monsoon
12	October 24, 2020	25.30644	82.20055	0	0	0	Monsoon
13	January 7, 2021	25.31785	83.0278	7.9	138.63	5.70	Nonmonsoon
13	January 11, 2021	25.17592	82.23135	0	0	0	Nonmonsoon
14	March 10, 2021	25.13694	82.75593	8.51	144.94	5.87	Nonmonsoon
14	March 14, 2021	25.32613	81.95671	0	0	0	Nonmonsoon
15	March 22, 2021	25.22757	82.5824	6.51	117.62	5.53	Nonmonsoon
15	March 26, 2021	25.32612	82.00888	0	0	0	Nonmonsoon
16	April 20, 2021	25.30761	83.01247	7.89	137.99	5.72	Nonmonsoon
16	April 24, 2021	25.17755	82.21987	0	0	0	Nonmonsoon

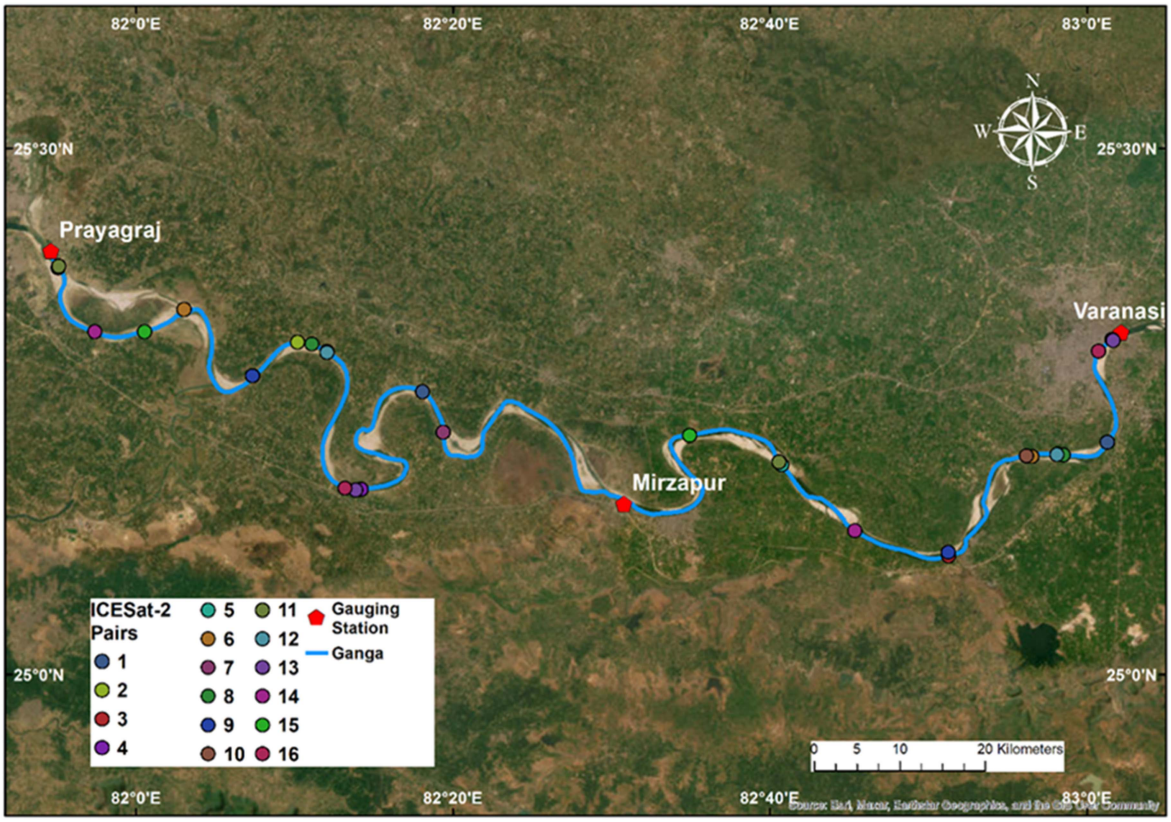

Fig. 4. ICESat-2 data pairs used for WSS estimation (refer to Table VI for more pairwise details).

TABLE VII
COMPARISON BETWEEN LONG-TERM SLOPES DERIVED FROM ICESAT-2 AND IN SITU GAUGES

Stations	Monsoon Slope (cm/km)	Non-Monsoon Slope (cm/km))
ICESat-2	5.16	5.74
In-situ Gauges	5.32	5.75
Mean absolute error MAE (In-situ – ICESat-2)	0.16	0.01

The WSS derived using ICESat-2 showed an average slope of 5.16 cm/km for the monsoon season, while 5.75 cm/km for the nonmonsoon season. As discerned from Table VII, there is negligible disparity between the slope estimated from in situ gauge stations and the ICESat-2 data. The closer alignment of WSS values between the in situ gauges and the ICESat-2 methods confirms the viability of ICESat-2 for WSS estimation. This suggests that the linear interpolation approach employed to extrapolate in situ time series to virtual stations for performance assessment is dependable, given the limitations associated with in situ gauges. Consequently, the mean slope derived from the CWC time series spanning 1980 to 2019, which equates to 5.9 cm/km, was utilized to project the in situ gauge time series onto virtual stations. The decrease in WSS during the monsoon season shows that as the water level rises in a river, the WSS tends to flatten out. Furthermore, channel-floodplain geometry governs the WSS during lean periods showing relatively higher WSS.

3) WSS Using ICESat-2 Data for SWORD River Reaches: For comparative assessment, the instantaneous WSS was calculated from ICESat-2 using its unique six beam configuration [58] corresponding to SWORD Ganga River reach IDs. The slope was calculated for a different period, between 2019 and 2022, which was then distributed between monsoon and nonmonsoon seasons. The river reach IDs from SWORD dataset allowed us to compare the WSS from the three sources: ICESat-2, Field GNSS, and the SWORD dataset (see Table VIII). The bias (GNSS- ICESat-2) range and mean between GNSS and ICESat-2 for SWORD reaches was found to be –3.72 to 2.27, 0.64 cm /km during nonmonsoon season and –5.9 to 4.42, 0.22 cm/km in monsoon season. Even though bias range was on higher side (because of few pairs highlighted in bold font which can be

TABLE VIII
COMPARISON OF WSS SLOPES FOR SWORD REACH IDS ALONG THE GANGA RIVER

SWORD Reach	ICESat-2 Non-monsoon (cm/km)	GNSS-based during April, 2023 (cm/km)	ICESat-2 Monsoon (cm/km)	GNSS-based during October, 2023 (cm/km)	SWORD Data (cm/km)
45245700041	–	2.94	4.09	5.85	9.21
45245700051	2.41	3.78	4.34	4.91	24.13
45245700071	2.17	2.35	3.52	3.84	4.94
45245700081	4.00	7.20	–	3.74	1.31
45245700091	***10.5***	***6.78***	***5.02***	***9.44***	12.73
45245700111	2.50	2.39	–	4.24	0.66
45245700131	3.59	5.29	–	6.02	18.52
45245700141	5.85	6.00	4.61	4.70	1.21
45245700151	4.46	4.41	–	4.73	0.46
45245700161	3.75	4.43	–	4.74	1.59
45245700171	–	1.58	1.68	4.28	0.00
45245700181	2.72	3.15	***17.0***	***11.10***	2.81
45245700191	–	2.49	2.49	4.86	8.95
45245900011	*8.53*	*10.2*	–	*6.58*	12.25
45245900021	9.23	11.50	12.9	8.70	0.00

Note: "-" indicates nonavailability of data or data gaps for given river reach.

considered as outliers), relatively low mean bias for both seasons and reach wise inspection assures the potential of ICESat-2 to capture the spatial and seasonal variability of the WSS.

In order to verify the statistical robustness of the SWORD WSS, averages of GNNS and ICESat-2 slopes from both seasons were considered for only reaches where non-zero slopes were available in the SWORD database. Results show that the bias (GNSS- SWORD) varies between –19.78 and 4.3 cm/km having a mean of –2.3 cm/km when compared to GNSS data. Furthermore, when compared with ICESat-2 slopes (5 sample points), bias (SWORD- ICESat-2) range and mean found to be –4.02 to 20.76 and 4.5 cm/km, respectively. It is observed that SWORD dataset showed relatively low agreement with GNSS and ICESat-2 data; obviously because of higher vertical accuracy of the ICESat-2 data compared to MERIT DEM [36]. Furthermore, Scherer et al. [36] compared ICESat-2 river surface slope (IRIS) with SWORD, and reported the bias range from –65.7 to 477.4 cm/km on basin scale (having reaches more than 5) with mean of 14.9 cm/km. The proposed statistics unfolds the advantage and limitations of the SWORD WSS slope using available limited in-situ and satellite observations. This will have direct impacts on the accuracy of SWOT products. The reason can be attributed to the fact that the SWORD WSS is based on the MERIT HydroDEM and time gap with reference to other sources of the data [37], [59].

V. DISCUSSION

A. Performance Comparison of Radar and LiDAR Altimetry Data

This study examines radar altimeter observations spanning from the ENVISAT mission's launch in 2002 to the ongoing Sentinel-3 mission. The accuracy of river water level measurements obtained through these missions is evaluated and compared to findings from prior research efforts. Notably, radar altimeters consistently align with previous studies [12], [16], [23], [42], [56]. [38] assessed ENVISAT and Jason-2 data for medium-width rivers (200 m or less) and found remarkably low RMSE values of 0.5 m and 0.2 cm, respectively. In contrast, for the Ganga River, the lowest RMSE recorded was 0.34 m for

ENVISAT and 1.11 m for Jason-2. The higher RMSE for Jason-2 can be attributed to its relatively larger 20 km footprint. Another study in the White Volta River basin in Ghana reported a higher RMSE ranging from 1.50 to 1.85 m for Jason-2 in monthly evaluations [60]. [61] assessed the Ogooué river basin in Gabon, Central Africa, and reported RMSE values lower than 0.48 m and 0.33 m for ENVISAT and Saral/AltiKa, respectively, at 16 virtual stations (compared to one in-situ gauging station). In the current study, Saral/AltiKa showed a slightly higher anomaly with an average RMSE of 0.77 m when compared to previous works [9], [38], [61]. Despite Saral's advantages over previous missions, such as a high PRF of 500 MHz and an 8 km footprint, its lower performance could be attributed to the small observation size and characteristics of the river channel-floodplain system.

Consistent with prior research, the Sentinel-3 mission outperformed all previous missions due to its SAR mode, which allows for a high along-track resolution of 300 m [41], [62], [63], [64].

Generally, results obtained from missions operating in LRM were surpassed by those from Sentinel-3's SAR acquisition mode. In addition, all missions, regardless of their instrument configurations, effectively captured seasonal variations in water levels at ten virtual stations. This highlights the potential to study the impacts of climate change and human interventions on the hydrological response of river basins. Although we were unable to compare seasonal statistics with previous studies for other global river basins due to a lack of validation, this study presents a foundational assessment of radar altimetry dataset performance in characterizing seasonal changes in river water levels.

The evaluation outcomes from ICESat revealed an RMSE of 0.82 m at the scale of the Ganga River (refer to Table III). This level of accuracy falls on the lower side when compared with previous investigations. For instance, Xiang et al. [28] reported an RMSE of 0.24 m for the Mississippi River, while Hall et al. [65] found a mean absolute error of 0.19 m between gauge station and ICESat water levels in the Mississippi River. This slight deviation is likely attributed to the mission's nonrepeating nature, varying water surface slope, a relatively small sample size (14 or fewer data points), and interpolation of in situ water levels. On the other hand, the assessment results for ICESat-2 exhibited an RMSE of 0.64 m at the river scale (as detailed in Table III), accompanied by higher values of R^2 (0.97) and NSE (0.97). However, the validation of ICESat-2 over the Ganga River was considerably limited due to the recent release of data, resulting in just 19 sample points. A relatively weaker agreement was observed between ICESat-2 and in-situ water levels in comparison to assessments in the Mississippi River (RMSE 0.06 m) and the Mekong River (RMSE 0.24 m) [28], [66]. The likely reasons for such variations include the influence of changing water surface slope and water waves, a small sample size, and the interpolation of in situ water levels at virtual stations. While this study did not specifically address the measurement precision between strong beam and weak beam data, previous research did not discover significant variations resulting in RMSE differences of 0.01 m in the Mekong River [66], 0.005 m in the Mississippi River [28], and 0.05 min Nath Sagar Reservoir, India [67]. Remarkably, ICESat-2 exhibited very promising outcomes for WSS estimation, demonstrating strong agreement with GNNS and in situ water level-based slope estimations. Consequently, the adoption of the IRIS product [36] is expected to significantly enhance the accuracy of SWOT discharge products. It is important to note that very few studies have conducted evaluations of ICESat-2 over rivers. Thus, this present study serves as an early performance evaluation of ICESat-2 for river applications.

B. Implications for Hydrological Applications

In hydrology, the use of satellite altimetry is not a recent development [22], [68], [69], although its adoption began with its application in oceanography for sea level monitoring. A multitude of applications are readily accessible for rivers and lakes, with some still in the development phase, taking advantage of advancements in computational capabilities and the continuous evolution of earth observation satellite configurations.

The primary application of altimetry datasets lies in the monitoring of water levels in rivers and lakes, which in turn unveils the seasonal dynamics of river basins. Our assessment of radar altimeters from various satellites unveiled the efficiency of the generated water level data in capturing the seasonal variations in the Ganga River's water levels, irrespective of sensor configurations and spatial–temporal resolutions. The relatively coarse temporal sampling of laser altimeters limits their applicability for tracking water level dynamics in rivers. In contrast, laser altimeters have demonstrated promising results in lake studies due to the possibility of increasing observation frequency by considering a higher number of observations within a certain radius of the station, along with the high density of tracks and minimal spatial variability in water levels [28], [70]. Another valuable application of altimetry-derived water levels is their role in calibrating and validating hydrodynamic models, especially in sparsely gauged or ungauged river basins. Extensive efforts have been devoted to evaluating multimission satellite altimetry data and assessing the impacts of their spatial and temporal resolutions on model calibration and validation [17], [19], [71]. Altimeter data have also been employed to understand river channel–floodplain interactions [72], [73], conduct wetland studies [74], [75], and estimate river roughness coefficients [55].

Concurrent with the generation of water level time-series, the hydrological community has been deeply engrossed in deciphering how to translate altimetry-based water levels into river discharge (for comprehensive insights, refer to [8], [76], [77], [78], and references therein). Moreover, considerable attention has been dedicated to the characterization of WSS, which can be employed, in conjunction with other parameters like river water level, river width, and river travel time, for the estimation of river discharge through diverse algorithms. In this context, we have demonstrated that ICESat-2 data can be harnessed to estimate WSS, which exhibits seasonal variations. Furthermore, numerous discharge algorithms that are being identified for generating global SWOT discharge product encompass WSS as a pivotal component [8]. River slope plays a crucial role in these algorithms, facilitating the estimation of time-invariant parameters such as river bathymetry and coefficients governing hydraulic resistance through the utilization of flow law

parameters estimation techniques as well as data assimilation approaches (as elaborated in [8]).

VI. Conclusion

In this study, we conducted the first comprehensive evaluation of combined radar (ENVISAT to Sentinel-3) and LiDAR (ICESat, ICESat-2) altimeter data over the Ganga River, stretching from Prayagraj to Varanasi, using long-term water level data from gauging stations and continuous water surface elevation data collected in the field. The performance of radar altimeters, with their varying instrument configurations, was compared and validated against in-situ data to generate water level time-series and characterize seasonal water level changes. For LiDAR altimeters, the assessment focused on evaluating water level dynamics and estimating WSS. The conclusions drawn from our results and discussions are as follows.

1) Across ten virtual stations, all radar altimeters from ENVISAT to Sentinel-3 displayed superior performance in comparison to in situ data ($R^2 > 0.8$; RMSE ranging from 0.11 to 1.16 m). As observed in previous studies, Sentinel-3 showcased the highest performance, potentially attributed to its data acquisition capability in SAR mode (RMSE ranging from 0.11 to 0.14 cm).
2) Present work unravels the first statistical assessment of radar altimeters to capture the seasonal water level change. We found that spaceborne radar altimeters with varying observation time-period were able to reproduce observed change in water level from premonsoon to monsoon season with RMSE of 0.59 m.
3) In general, ICESat-2 (RMSE on river scale: 0.64 m; R^2 0.97) showed better performance compared to ICESat (average RMSE of nine virtual stations: 0.82 m; $R^2 >= 0.6$ only for three stations) for retrieved water levels. While LiDAR altimeters excel in vertical accuracy, their coarse temporal resolution characteristics may pose some challenges in accurately capturing high fluctuations in river water levels.
4) WSS slope estimated using ICESat-2 data on river scale showed better agreement with long-term gauged data during both monsoon (MAE 0.16 cm/km) and nonmonsoon season (MAE 0.01 cm/km). At the same time, relatively low mean bias (GNSS- ICESat-2) was observed between ICESat-2 and GNSS slopes corresponding to SWORD reaches during monsoon season (0.22 cm/km) and nonmonsoon season (0.64 cm /km). This validates the potential of ICESat-2 to capture the spatial and seasonal variability of the WSS.
5) Based on limited concurrent readings, SWORD WSS showed relatively low agreement with the GNSS and ICESat-2 data. Thus, utilization of the IRIS (currently available only Europe and North America; [36]) can improve the accuracy of SWOT discharge products.
6) This study introduces a foundational assessment of the collective performance of radar and LiDAR altimeters for Ganga River. This assessment targets end users engaged in extracting river water levels from ungauged sites, catering to diverse hydrological applications including river discharge estimation. Furthermore, the study site closely follows the calibration orbit of the SWOT mission, making the results applicable for evaluating SWOT mission measurements.

Acknowledgment

The authors would like to thank Inland Waterways Authority of India (IWAI) and Central Water Commission (CWC), India, for providing significant support in field work. The authors are grateful to Hydroweb, Center for Topographic Studies of the Ocean and Hydrosphere (CTOH) and NSIDC for providing radar and LiDAR altimetry data, and CWC for providing in situ gauging data. The authors also sincerely thank the authorities of Indian Space Research Organisation (ISRO), Indian Institute of Technology, Roorkee and Institut de Recherche pour le Développement (IRD), France for the financial support and providing all the facilities to carry out this work. The radar altimetry can be downloaded from the https://hydroweb.theia-land.fr and https://ctoh.legos.obs-mip.fr/applications/land_surfaces/altimetric_data/altis. The LiDAR altimetry data can be downloaded from the OpenAltimetry (https://openaltimetry.org/) and https://nsidc.org/data. The raw in situ data used in the present work can be requested from the website https://59.179.30.67:94/ as Ganga River comes under classified data category and it is not-transferable to third party. The AlTis software used in the present work can be downloaded from the https://gitlab.com/ctoh/altis. The authors declare that they have no known competing financial interests or personal relationships that could have influenced the work reported in this article.

References

[1] J. F. Pekel, A. Cottam, N. Gorelick, and A. S. Belward, "High-resolution mapping of global surface water and its long-term changes," *Nature*, vol. 540, no. 7633, pp. 418–422, 2016, doi: 10.1038/nature20584.
[2] D. M. Hannah et al., "Large-scale river flow archives: Importance, current status and future needs," *Hydrological Processes*, vol. 25, no. 7, pp. 1191–1200, 2011, doi: 10.1002/hyp.7794.
[3] F. Hossain et al., "Proof of concept of an altimeter-based river forecasting system for transboundary flow inside Bangladesh," *IEEE J. Sel. Topics Appl. Earth Observ. Remote Sens.*, vol. 7, no. 2, pp. 587–601, Feb. 2014.
[4] P. R. Dhote, Y. Joshi, A. Rajib, P. K. Thakur, B. R. Nikam, and S. P. Aggarwal, "Evaluating topography-based approaches for fast floodplain mapping in data-scarce complex-terrain regions: Findings from a Himalayan Basin," *J. Hydrol.*, vol. 620, 2023, Art. no. 129309, doi: 10.1016/j.jhydrol.2023.129309.
[5] C. J. Vörösmarty, P. Green, J. Salisbury, and R. B. Lammers, "Global water resources: Vulnerability from climate change and population growth," *Science*, vol. 289, no. 5477, pp. 284–288, 2000, doi: 10.1126/science.289.5477.284.
[6] R. Lawford, A. Strauch, D. Toll, B. Fekete, and D. Cripe, "Earth observations for global water security," *Curr. Opin. Environ. Sustainability*, vol. 5, no. 6, pp. 633–643, 2013, doi: 10.1016/j.cosust.2013.11.009.
[7] S. Abdalla et al., "Altimetry for the future: Building on 25 years of progress," *Adv. Space Res.*, vol. 68, no. 2, pp. 319–363, 2021, doi: 10.1016/j.asr.2021.01.022.
[8] M. Durand et al., "A framework for estimating global river discharge from the surface water and ocean topography satellite mission," *Water Resour. Res.*, vol. 59, no. 4, Apr. 2023, Art. no. e2021WR031614, doi: 10.1029/2021WR031614.
[9] P. Bonnefond et al., "The benefits of the Ka-band as evidenced from the SARAL/AltiKa altimetric mission: Quality assessment and unique characteristics of AltiKa data," *Remote Sens.*, vol. 10, no. 1, 2018, Art. no. 83, doi: 10.3390/rs10010083.

[10] Y. B. Sulistioadi et al., "Satellite radar altimetry for monitoring small rivers and lakes in Indonesia," *Hydrol. Earth Syst. Sci.*, vol. 19, no. 1, pp. 341–359, 2015, doi: 10.5194/hess-19-341-2015.

[11] N. Taburet et al., "S3MPC: Improvement on inland water tracking and water level monitoring from the OLTC onboard Sentinel-3 altimeters," *Remote Sens.*, vol. 12, no. 18, 2020, Art. no. 3055, doi: 10.3390/POLYM12092146.

[12] S. Biancamaria et al., "Validation of Jason-3 tracking modes over French rivers," *Remote Sens. Environ.*, vol. 209, pp. 77–89, 2018, doi: 10.1016/j.rse.2018.02.037.

[13] M. J. Tourian et al., "Spatiotemporal densification of river water level time series by multimission satellite altimetry," *Water Resour. Res.*, vol. 52, no. 2, pp. 1140–1159, 2016, doi: 10.1002/2015WR017654.

[14] E. Boergens, S. Buhl, D. Dettmering, C. Klüppelberg, and F. Seitz, "Combination of multi-mission altimetry data along the Mekong river with spatio-temporal kriging," *J. Geodesy*, vol. 91, no. 5, pp. 519–534, 2017, doi: 10.1007/s00190-016-0980-z.

[15] K. Nielsen, E. Zakharova, A. Tarpanelli, O. B. Andersen, and J. Benveniste, "River levels from multi mission altimetry, a statistical approach," *Remote Sens. Environ.*, vol. 270, 2022, Art. no. 112876, doi: 10.1016/j.rse.2021.112876.

[16] A. A. Jarihani, J. N. Callow, K. Johansen, and B. Gouweleeuw, "Evaluation of multiple satellite altimetry data for studying inland water bodies and river floods," *J. Hydrol.*, vol. 505, pp. 78–90, 2013, doi: 10.1016/j.jhydrol.2013.09.010.

[17] P. R. Dhote et al., "The use of SARAL/AltiKa altimeter measurements for multi-site hydrodynamic model validation and rating curves estimation: An application to Brahmaputra river," *Adv. Space Res.*, vol. 68, no. 2, pp. 691–702, Jul. 2021, doi: 10.1016/j.asr.2020.05.012.

[18] A. Domeneghetti et al., "The use of remote sensing-derived water surface data for hydraulic model calibration," *Remote Sens. Environ.*, vol. 149, pp. 130–141, 2014, doi: 10.1016/j.rse.2014.04.007.

[19] A. Domeneghetti et al., "Testing the use of single- and multi-mission satellite altimetry for the calibration of hydraulic models," *Adv. Water Resour.*, vol. 151, May 2021, Art. no. 103887, doi: 10.1016/J.ADVWATRES.2021.103887.

[20] C. I. Michailovsky, C. Milzow, and P. Bauer-Gottwein, "Assimilation of radar altimetry to a routing model of the Brahmaputra River," *Water Resour. Res.*, vol. 49, no. 8, pp. 4807–4816, 2013, doi: 10.1002/wrcr.20345.

[21] A. K. Rai, Z. Beg, A. Singh, and K. Gaurav, "Estimating discharge of the Ganga river from satellite altimeter data," *J. Hydrol.*, vol. 603, 2021, Art. no. 126860, doi: 10.1016/j.jhydrol.2021.126860.

[22] C. M. Birkett, "Contribution of the TOPEX NASA radar altimeter to the global monitoring of large rivers and wetlands," *Water Resour. Res.*, vol. 34, no. 5, pp. 1223–1239, May 1998, doi: 10.1029/98WR00124.

[23] F. Frappart et al., "Preliminary assessment of SARAL/AltiKa observations over the Ganges-Brahmaputra and Irrawaddy rivers," *Mar. Geodesy*, vol. 38, pp. 568–580, 2015, doi: 10.1080/01490419.2014.990591.

[24] F. Papa et al., "Ganga-Brahmaputra river discharge from Jason-2 radar altimetry: An update to the long-term satellite-derived estimates of continental freshwater forcing flux into the Bay of Bengal," *J. Geophysical Res., Oceans*, vol. 117, no. 11, 2012, doi: 10.1029/2012JC008158.

[25] P. Li, H. Li, F. Chen, and X. Cai, "Monitoring long-term lake level variations in middle and lower Yangtze Basin over 2002-2017 through integration of multiple satellite altimetry datasets," *Remote Sens.*, vol. 12, no. 9, 2020, Art. no. 1448, doi: 10.3390/RS12091448.

[26] J. Chen and J. Liao, "Monitoring lake level changes in China using multi-altimeter data (2016–2019)," *J. Hydrol.*, vol. 590, 2020, Art. no. 125544, doi: 10.1016/j.jhydrol.2020.125544.

[27] D. Dettmering, C. Schwatke, E. Boergens, and F. Seitz, "Potential of ENVISAT radar altimetry for water level monitoring in the Pantanal wetland," *Remote Sens.*, vol. 8, no. 7, 2016, Art. no. 596, doi: 10.3390/rs8070596.

[28] J. Xiang, H. Li, J. Zhao, X. Cai, and P. Li, "Inland water level measurement from spaceborne laser altimetry: Validation and comparison of three missions over the Great Lakes and lower Mississippi River," *J. Hydrol.*, vol. 597, 2021, Art. no. 126312, doi: 10.1016/j.jhydrol.2021.126312.

[29] F. E. O'Loughlin, J. Neal, D. Yamazaki, and P. D. Bates, "ICESat-derived inland water surface spot heights," *Water Resour. Res.*, vol. 52, no. 4, pp. 3276–3284, 2016, doi: 10.1002/2015WR018237.

[30] N. Baghdadi, N. Lemarquand, H. Abdallah, and J. S. Bailly, "The relevance of GLAS/ICESat elevation data for the monitoring of river networks," *Remote Sens.*, vol. 3, no. 4, pp. 708–720, 2011, doi: 10.3390/rs3040708.

[31] V. H. Phan, R. Lindenbergh, and M. Menenti, "ICESat derived elevation changes of Tibetan lakes between 2003 and 2009," *Int. J. Appl. Earth Observ. Geoinf.*, vol. 17, no. 1, pp. 12–22, 2012, doi: 10.1016/j.jag.2011.09.015.

[32] B. E. Schutz, H. J. Zwally, C. A. Shuman, D. Hancock, and J. P. DiMarzio, "Overview of the ICESat mission," *Geophysical Res. Lett.*, vol. 32, no. 21, 2005, doi: 10.1029/2005GL024009.

[33] A. Neuenschwander, E. Guenther, J. C. White, L. Duncanson, and P. Montesano, "Validation of ICESat-2 terrain and canopy heights in boreal forests," *Remote Sens. Environ.*, vol. 251, 2020, Art. no. 112110, doi: 10.1016/j.rse.2020.112110.

[34] F. Frappart et al., "Evaluation of the performances of radar and LiDAR altimetry missions for water level retrievals in mountainous environment: The case of the Swiss lakes," *Remote Sens.*, vol. 13, no. 11, 2021, Art. no. 2196, doi: 10.3390/rs13112196.

[35] C. Yuan, P. Gong, and Y. Bai, "Performance assessment of ICESat-2 laser altimeter data for water-level measurement over lakes and reservoirs in China," *Remote Sens.*, vol. 12, no. 5, 2020, Art. no. 770, doi: 10.3390/rs12050770.

[36] D. Scherer, C. Schwatke, D. Dettmering, and F. Seitz, "ICESat-2 river surface slope (IRIS): A global reach-scale water surface slope dataset," *Sci. Data*, vol. 10, no. 1, Jun. 2023, Art. no. 359, doi: 10.1038/s41597-023-02215-x.

[37] E. H. Altenau, T. M. Pavelsky, M. T. Durand, X. Yang, R. P. de M. Frasson, and L. Bendezu, "The surface water and ocean topography (SWOT) mission river database (SWORD): A global river network for satellite data products," *Water Resour. Res.*, vol. 57, no. 7, Jul. 2021, Art. no. e2021WR030054, doi: 10.1029/2021WR030054.

[38] S. Biancamaria et al., "Satellite radar altimetry water elevations performance over a 200 m wide river: Evaluation over the Garonne river," *Adv. Space Res.*, vol. 59, no. 1, pp. 128–146, 2017, doi: 10.1016/j.asr.2016.10.008.

[39] A. K. Dubey, P. Gupta, S. Dutta, and B. Kumar, "Evaluation of satellite-altimetry-derived river stage variation for the braided Brahmaputra river," *Int. J Remote Sens.*, vol. 35, no. 23, pp. 7815–7827, 2014, doi: 10.1080/01431161.2014.978033.

[40] R. Schneider, A. Tarpanelli, K. Nielsen, H. Madsen, and P. Bauer-Gottwein, "Evaluation of multi-mode CryoSat-2 altimetry data over the Po river against in situ data and a hydrodynamic model," *Adv. Water Resour.*, vol. 112, pp. 17–26, 2018, doi: 10.1016/j.advwatres.2017.11.027.

[41] C. M. M. Kittel, L. Jiang, C. Tøttrup, and P. Bauer-Gottwein, "Sentinel-3 radar altimetry for river monitoring - A catchment-scale evaluation of satellite water surface elevation from Sentinel-3A and Sentinel-3B," *Hydrol. Earth Syst. Sci.*, vol. 25, no. 1, pp. 333–357, 2021, doi: 10.5194/hess-25-333-2021.

[42] J. Chen et al., "Evaluation of Sentinel-3A altimetry over Songhua river Basin," *J. Hydrol.*, vol. 618, Mar. 2023, Art. no. 129197, doi: 10.1016/J.JHYDROL.2023.129197.

[43] H. Li, J. Zhang, X. Cai, H. Huang, and L. Wang, "On the capacity of ICESat-2 laser altimetry for river level retrieval: An investigation in the Ohio river Basin," *J. Hydrol.*, vol. 626, Nov. 2023, Art. no. 130277, doi: 10.1016/j.jhydrol.2023.130277.

[44] CWC & NRSC, "Ganga river Basin report prepared by central water commission (CWC) and national remote sensing centre (NRSC), ISRO," 2014.

[45] D. Kumar, "River Ganges–Historical, cultural and socioeconomic attributes," *Aquatic Ecosyst. Health Manage.*, vol. 20, nos. 1/2, pp. 8–20, Apr. 2017, doi: 10.1080/14634988.2017.1304129.

[46] CTOH, "Center for topographic studies of the ocean and hydrosphere," Accessed: Jan. 4, 2022. [Online]. Available: https://ctoh.legos.obs-mip.fr/

[47] F. Frappart, S. Calmant, M. Cauhope, F. Seyler, and A. Cazenave, "Preliminary results of ENVISAT RA-2-derived water levels validation over the Amazon Basin," *Remote Sens. Environ.*, vol. 100, no. 2, pp. 252–264, Jan. 2006, doi: 10.1016/j.rse.2005.10.027.

[48] J. S. da Silva, S. Calmant, F. Seyler, O. C. R. Filho, G. Cochonneau, and W. J. Mansur, "Water levels in the Amazon Basin derived from the ERS 2 and ENVISAT radar altimetry missions," *Remote Sens. Environ.*, vol. 114, no. 10, pp. 2160–2181, Oct. 2010, doi: 10.1016/j.rse.2010.04.020.

[49] J.-F. Crétaux et al., "Absolute calibration or validation of the altimeters on the Sentinel-3A and the Jason-3 over Lake Issykkul (Kyrgyzstan)," *Remote Sens.*, vol. 10, no. 11, Oct. 2018, Art. no. 1679, doi: 10.3390/rs10111679.

[50] H. J. Zwally et al., "ICESat's laser measurements of polar ice, atmosphere, ocean, and land," *J. Geodyn.*, vol. 34, nos. 3/4, pp. 405–445, Oct. 2002, doi: 10.1016/S0264-3707(02)00042-X.

[51] J. B. Abshire et al., "Geoscience laser altimeter system (GLAS) on the ICESat Mission: On-orbit measurement performance," *Geophysical Res. Lett.*, vol. 32, no. 21, 2005, Art. no. L21S02, doi: 10.1029/2005GL024028.

[52] T. Markus et al., "The ice, cloud, and land elevation Satellite-2 (ICESat-2): Science requirements, concept, and implementation," *Remote Sens. Environ.*, vol. 190, pp. 260–273, Mar. 2017, doi: 10.1016/j.rse.2016.12.029.

[53] J.-F. Crétaux et al., "SOLS: A lake database to monitor in the near real time water level and storage variations from remote sensing data," *Adv. Space Res.*, vol. 47, no. 9, pp. 1497–1507, May 2011, doi: 10.1016/j.asr.2011.01.004.

[54] S. J. S. Khalsa et al., "OpenAltimetry - rapid analysis and visualization of spaceborne altimeter data," *Earth Sci. Informat.*, vol. 15, no. 3, pp. 1471–1480, Sep. 2022, doi: 10.1007/s12145-020-00520-2.

[55] A. K. Dubey, V. Chembolu, and S. Dutta, "Utilization of satellite altimetry retrieved river roughness properties in hydraulic flow modelling of braided river system," *Int. J. River Basin Manage.*, vol. 20, no. 3, pp. 411–424, Jul. 2022, doi: 10.1080/15715124.2020.1830785.

[56] C. Normandin et al., "Evolution of the performances of radar altimetry missions from ERS-2 to Sentinel-3A over the Inner Niger Delta," *Remote Sens.*, vol. 10, no. 6, p. 833, May 2018, doi: 10.3390/rs10060833.

[57] G. LeFavour and D. Alsdorf, "Water slope and discharge in the Amazon River estimated using the shuttle radar topography mission digital elevation model," *Geophysical Res. Lett.*, vol. 32, no. 17, 2005, doi: 10.1029/2005GL023836.

[58] D. Scherer, C. Schwatke, D. Dettmering, and F. Seitz, "ICESat-2 based river surface slope and its impact on water level time series from satellite altimetry," *Water Resour. Res.*, vol. 58, no. 11, Nov. 2022, Art. no. e2022WR032842, doi: 10.1029/2022WR032842.

[59] D. Yamazaki, D. Ikeshima, J. Sosa, P. D. Bates, G. H. Allen, and T. M. Pavelsky, "MERIT hydro: A high-resolution global hydrography map based on latest topography dataset," *Water Resour. Res.*, vol. 55, no. 6, pp. 5053–5073, Jun. 2019, doi: 10.1029/2019WR024873.

[60] S. Darko, K. A. Adjei, C. Gyamfi, and S. N. Odai, "Statistical evaluation of Jason-2 satellite altimetry products in a trans-boundary river Basin; the case study of the White Volta river Basin in Ghana," *Model. Earth Syst. Environ.*, vol. 9, no. 2, pp. 2905–2917, 2023, doi: 10.1007/s40808-022-01655-5.

[61] S. Bogning et al., "Monitoring water levels and discharges using radar altimetry in an ungauged river Basin: The case of the Ogooué," *Remote Sens.*, vol. 10, no. 3, p. 350, Feb. 2018, doi: 10.3390/rs10020350.

[62] Q. Huang, X. D. Li, P. F. Han, D. Long, F. Y. Zhao, and A. Z. Hou, "Validation and application of water levels derived from Sentinel-3A for the Brahmaputra River," *Sci. China Technol. Sci.*, vol. 62, no. 10, pp. 1760–1772, 2019, doi: 10.1007/s11431-019-9535-3.

[63] A. Z. Zaidi et al., "Indus river water level monitoring using satellite radar altimetry," *Adv. Space Res.*, vol. 68, no. 2, pp. 641–651, 2021, doi: 10.1016/j.asr.2020.03.044.

[64] M. Halicki and T. Niedzielski, "The accuracy of the Sentinel-3A altimetry over Polish rivers," *J. Hydrol.*, vol. 606, 2022, Art. no. 127355, doi: 10.1016/j.jhydrol.2021.127355.

[65] A. C. Hall, G. J. P. Schumann, J. L. Bamber, P. D. Bates, and M. A. Trigg, "Geodetic corrections to Amazon river water level gauges using ICESat altimetry," *Water Resour. Res.*, vol. 48, no. 6, 2012, doi: 10.1029/2011WR010895.

[66] J. Lao, C. Wang, S. Nie, X. Xi, and J. Wang, "Monitoring and analysis of water level changes in Mekong river from ICESat-2 spaceborne laser altimetry," *Water*, vol. 14, no. 10, 2022, Art. no. 1613, doi: 10.3390/w14101613.

[67] G. Dandabathula and S. S. Rao, "Validation of ICESat-2 surface water level product ATL13 with near real time gauge data," *Hydrology*, vol. 8, no. 2, pp. 19–25, 2020, doi: 10.11648/j.hyd.20200802.11.

[68] C. M. Birkett, "Radar altimetry: A new concept in monitoring lake level changes," *Eos, Trans. Amer. Geophysical Union*, vol. 75, no. 24, p. 273, 1994, doi: 10.1029/94EO00944.

[69] S. Calmant and F. Seyler, "Continental surface waters from satellite altimetry," *Comptes Rendus Geosci.*, vol. 338, nos. 14/15, pp. 1113–1122, Nov. 2006, doi: 10.1016/j.crte.2006.05.012.

[70] S. Liu, Q. G. Jiang, X. S. Zhang, and K. G. Zhao, "Potential and limitations of satellite laser altimetry for monitoring water surface dynamics: ICESat for US lakes," *Int. J. Agricultural Biol. Eng.*, vol. 10, no. 5, pp. 154–165, 2017.

[71] A. C. V. Getirana, A. Boone, D. Yamazaki, and N. Mognard, "Automatic parameterization of a flow routing scheme driven by radar altimetry data: Evaluation in the Amazon Basin," *Water Resour. Res.*, vol. 49, no. 1, pp. 614–629, Jan. 2013, doi: 10.1002/wrcr.20077.

[72] A. Ovando, J. M. Martinez, J. Tomasella, D. A. Rodriguez, and C. von Randow, "Multi-temporal flood mapping and satellite altimetry used to evaluate the flood dynamics of the Bolivian Amazon wetlands," *Int. J. Appl. Earth Observ. Geoinf.*, vol. 69, pp. 27–40, Jul. 2018, doi: 10.1016/j.jag.2018.02.013.

[73] E. Park, "Characterizing channel-floodplain connectivity using satellite altimetry: Mechanism, hydrogeomorphic control, and sediment budget," *Remote Sens. Environ.*, vol. 243, Jun. 2020, Art. no. 111783, doi: 10.1016/j.rse.2020.111783.

[74] E. A. Zakharova, A. V. Kouraev, F. Rémy, V. A. Zemtsov, and S. N. Kirpotin, "Seasonal variability of the Western Siberia wetlands from satellite radar altimetry," *J. Hydrol.*, vol. 512, pp. 366–378, May 2014, doi: 10.1016/j.jhydrol.2014.03.002.

[75] V. Chembolu, A. K. Dubey, P. K. Gupta, S. Dutta, and R. P. Singh, "Application of satellite altimetry in understanding river–wetland flow interactions of Kosi river," *J. Earth Syst. Sci.*, vol. 128, no. 4, p. 89, Jun. 2019, doi: 10.1007/s12040-019-1099-4.

[76] I. Gejadze, P.-O. Malaterre, H. Oubanas, and V. Shutyaev, "A new robust discharge estimation method applied in the context of SWOT satellite data processing," *J. Hydrol.*, vol. 610, Jul. 2022, Art. no. 127909, doi: 10.1016/j.jhydrol.2022.127909.

[77] H. Oubanas, I. Gejadze, P. O. Malaterre, and F. Mercier, "River discharge estimation from synthetic SWOT-type observations using variational data assimilation and the full Saint-Venant hydraulic model," *J. Hydrol.*, vol. 559, pp. 638–647, 2018, doi: 10.1016/j.jhydrol.2018.02.004.

[78] C. Gleason and M. Durand, "Remote sensing of river discharge: A review and a framing for the discipline," *Remote Sens.*, vol. 12, no. 7, Mar. 2020, Art. no. 1107, doi: 10.3390/rs12071107.